ON THE IMPACT OF GLACIER ALBEDO UNDER CONDITIONS OF EXTREME GLACIER MELT: THE SUMMER OF 2003 IN THE ALPS

Frank Paul, Horst Machguth and Andreas Kääb

University of Zurich, Department of Geography, Zurich, Switzerland;
fpaul(at)geo.unizh.ch

ABSTRACT

The extraordinarily hot summer of 2003 caused record-breaking glacier melt in the European Alps (i.e. eight times the long-term average). Multispectral Landsat Thematic Mapper (TM) satellite data of August 2003 clearly shows very dark glacier ablation areas, particularly in the near-infrared. In order to assess the influence of the low glacier albedo and the special 2003 meteorological conditions on glacier mass balance more quantitatively, we have calculated glacier albedo from TM for three distinct years (1985, 1998, 2003) and applied a distributed glacier mass balance model forced by climatic mean as well as the special 2002/03 meteorological conditions. For this purpose, we use the TM-derived albedo for 1998 and 2003 as a surrogate for the background glacier albedo. We observe a large albedo variability from year to year, constant or even decreasing albedo with altitude and much lower albedo values in the ablation area than generally applied (0.15 instead of 0.35). The modelled mass balance reveals a distribution pattern that is governed by the potential solar radiation, increasing glacier mass loss with altitude using the 2003 albedo, and a three times higher mass loss for the meteorological conditions of 2002/03 compared to the climatic means.

Keywords: Glacier albedo, mass balance model, summer 2003.

INTRODUCTION

Discharge of meltwater from glaciers is an important water resource in many parts of the world (e.g. 1,2). In contrast to springtime snow-melt runoff, glaciers have their highest discharge in the hot summer months, when water is mostly needed (e.g. for irrigation). In the Alps, also called the 'water tower' of Europe, glacier melt can make a significant contribution to overall discharge, in particular during dry and hot summers (e.g. 3). Accordingly, the extraordinary heat wave of the summer 2003 (4) caused record breaking glacier melt with a corresponding mean specific mass loss of -2.5 m water equivalent (we), which is eight times the annual mean of the period 1960-2000 (5).

Glacier melt can be calculated from so-called distributed glacier mass balance models, which utilize a digital elevation model (DEM) to 'distribute' measured meteorological input variables (e.g. temperature, precipitation) to the topography by means of elevation-dependent lapse rates and DEM modelling for incoming solar radiation (e.g. 6,7,8). Such models have proven to calculate mass balance or discharge at well calibrated sites from a prescribed meteorological forcing very accurately (e.g. 9). Several field studies (e.g. 10,11,12) have confirmed that direct radiation is the most important energy source for glacier melt in the rough topography of the Alps. This is also due to the long ablation period (sometimes exceeding 90 days) and the comparably low albedo of bare glacier ice (about 0.3). As such, glacier albedo becomes the most sensitive variable for glacier melt. However, glacier albedo exhibits a high temporal (e.g. retreat of the snow line) and spatial (e.g. debris cover) variability. Thus, if glacier melt is to be assessed by a mass balance model over large regions, the usage of a glacier-specific albedo is most valuable. The spatial pattern of the albedo can be obtained from multispectral Landsat Thematic Mapper (TM) data over large regions with high accuracy (e.g. 13). However, acquisition at the end of the ablation period in a year with a minimum amount of remaining snow is mandatory.

In the study presented here, we compare TM-derived albedo values for several glaciers and three distinct years (1985, 1998, 2003) and assess the influence of the albedo on glacier mass balance and melt with a distributed mass balance model that is forced by the 2002/2003 balance year meteorological conditions (temperature, precipitation, clouds) as well as climatic mean values.

TEST SITE AND SNOW CONDITIONS

We have investigated three Landsat TM scenes (path: 195, row: 28) of 28 September 1985, 31 August 1998 and 13 August 2003 covering the south-western part of Switzerland. The specific ice and snow conditions of each respective year are shown for a test site (11 km by 7 km in size) in the Wildstrubel region in Figure 1. The three images illustrate very different surface conditions in the three years. While (Figure 1a) a snow-covered accumulation area (white to light grey) can be clearly distinguished from the snow-free ablation area (blue-grey) on most glaciers in 1985, Plaine Morte glacier (P) was nearly completely free of snow in 1998 and 2003 (Figure 1b and c), with a much darker blue-grey surface in 2003 (Figure 1c) as compared to 1998. On the other hand, Wildstrubel glacier (W) has a well-defined accumulation area in both years, with little more but much brighter snow in 2003. A similar melt pattern in the three years is found for most other glaciers within the three Landsat scenes. Figure 1d is a perspective view of the area (as seen from NNE) for illustration of the topographic conditions of the test site. In particular the 9.1 km^2 sized Plaine Morte glacier is mostly flat and, thus, its net balance is very sensitive to small shifts of the equilibrium line altitude (ELA).

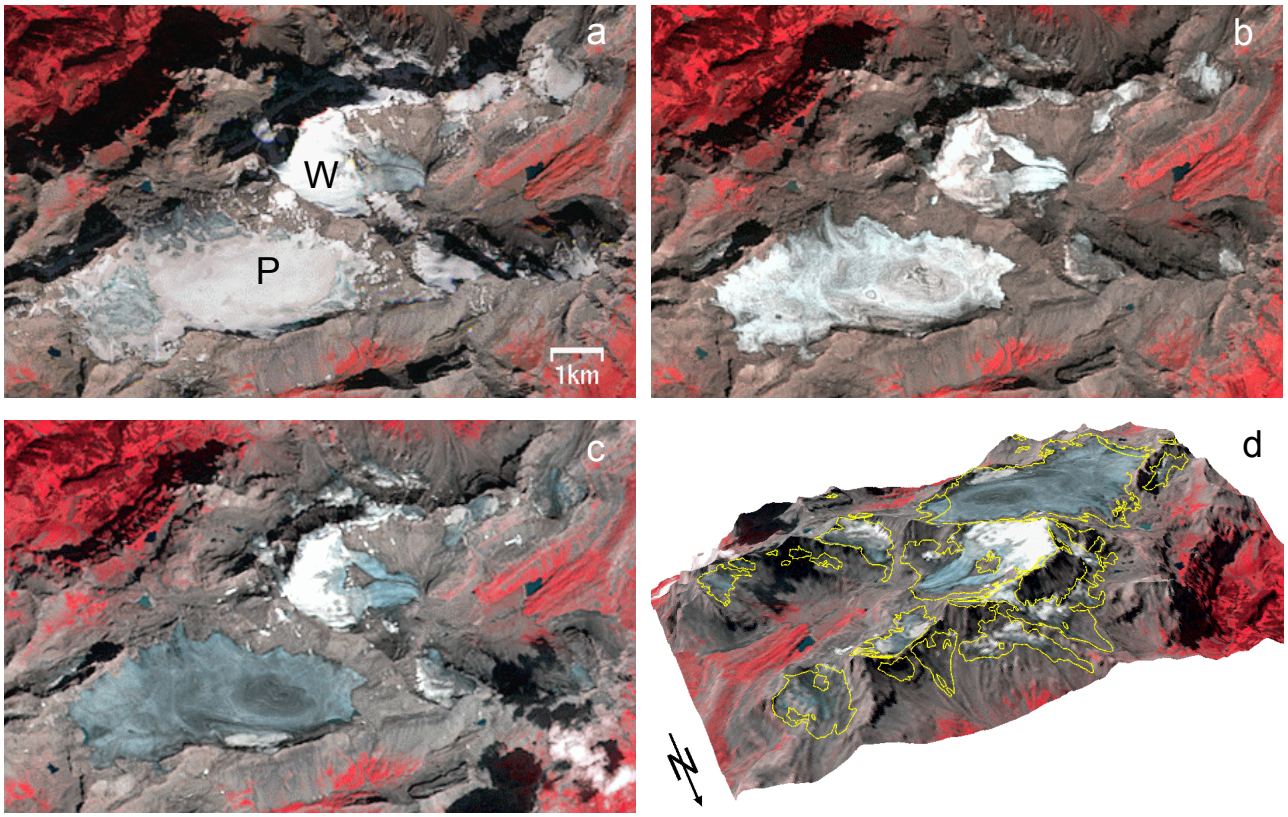

Figure 1: TM band 4, 3, 2 composites of the test site with north at top (glaciers: P=Plaine Morte, W=Wildstrubel). a) Conditions in 1985, b) in 1998 and, c) in 2003. d) Perspective view with the 2003 scene and 1973 glacier outlines (yellow) draped over the DEM25 (© 2003 swisstopo, BA057049).

In other regions, a very dark zone is visible directly below the snow line in 1998 and 2003 on many larger glaciers. It can be related to dirty firn areas from previous summers. Moreover, the higher reflection of the bare ice regions of all glaciers in 1998 is outstanding in comparison to 2003. However, in absolute terms they are not much brighter than in 1985 (see below).

The meteorological conditions in the three investigated years were also quite different from each other. In 1985, a larger than average winter snowpack was not largely reduced during an average summer (with cold and rainy spells in July and August), while the summer of 1998 was very long, dry and warm, and melted most of the winter snow pack which had a normal thickness. The brownish hue (Figure 1b) of the snow results from a Saharan dust-fall event in spring. The extraordinarily hot and dry summer of 2003 (heat waves in June and August, little precipitation) had melted most of the larger than average snow pack by mid-August (meteorological conditions from Meteoswiss).

SATELLITE DERIVED GLACIER ALBEDO

All Landsat scenes are orthorectified with a large number of ground control points (>30) and the DEM25 level 2 from swisstopo to a positional accuracy of about one pixel (*RMSE* < 25 m) using the Orthoengine software package from PCI geomatica. In order to apply the narrowband to broadband albedo conversion for snow and ice as developed by (13), we have applied the RCOR2 atmospheric / topographic correction method (14). For our study we select a standard atmospheric profile (mid latitude summer with continental type aerosol) and horizontal visibilities for six specific elevation levels (from 500 to 3500 m) to describe atmospheric conditions. The related correction is taken from an atmospheric catalogue (look-up-table) that was computed from the 6S radiative transfer code (15).

The atmospheric conditions are considered to be constant over the entire scene and in all three years; of course, in particular the latter is not the case. However, as we study mostly regions above 2000 m a.s.l. and reported visibilities exceed 40 km above 1500 m in all three years, the atmospheric influence is small. Much more important is the correct position of the DEM with respect to the satellite image, in order to reduce artefacts of over- or under-correction along mountain crests.

The RCOR2 module considers sky-view and terrain-view factors (obtained from the DEM) as well as local illumination (scaled cosine of the local solar incidence angle) and a map of regions in cast shadow for the time of the satellite overpass. Gain and offset coefficients for conversion of digital numbers (DN) into radiances are taken from PCI geomatica and held constant, as they have proven to give accurate results with RCOR2 (14). The RCOR2 module provides spectral reflectance at the satellite sensor (R_λ) for each respective band λ and was converted to broadband glacier albedo (A_G) according to (13) using:

$$A_G = 0.726\,R_{TM2} - 0.322\,R_{TM2}^2 - 0.051 R_{TM4} + 0.581 R_{TM4}^2$$

Several studies (e.g. 16) have confirmed the accuracy of the equation given above for snow and ice surfaces from simultaneous field measurements. However, with decreasing solar elevation the bi-directional reflectance distribution function (*BRDF*) becomes increasingly important, as ice and snow exhibit a forward scattering component (17). We neglect the *BRDF* in our calculation for several reasons: (i) The very complex calculations (taking slope and aspect of each pixel into account) are beyond the scope of this paper, (ii) surface properties may vary strongly at a local scale (impurities, liquid water content, etc.), and (iii) the possible correction (up to +0.1) is still within the range of errors due to other assumptions made (e.g. see above). The equation for the glacier albedo (A_G) is only applied to debris-free glacier regions that are obtained beforehand from a thresholded TM3 / TM5 ratio image with an additional threshold in TM1 to discriminate ice and snow from rock in regions of cast shadow (e.g. 18). For all other regions of the image, a rock albedo (A_R) was calculated according to (19):

$$A_R = 0.493\,R_{TM2} + 0.507\,R_{TM4}$$

COMPARISON OF GLACIER ALBEDO VALUES

In Figure 2 we show the albedo values obtained for the three years and the Wildstrubel test site (cf. Figure 1). Apart from obvious artefacts along mountain crests or in regions of cast shadow the

topographic normalization was quite successful, as effects of illumination due to the topography have been removed and all images appear flat (Figure 2). However, some regions remain un- or over corrected. Large differences in glacier albedo are visible from year to year. In particular the high bare ice albedo of Plaine Morte glacier in 1998 (Figure 2b) compared to the low albedo in 2003 (Figure 2c) is remarkable. Moreover, snow in the accumulation area appears much darker in 1998 than in 2003 or 1985. However, as we found nearly identical albedo values for bare rock surfaces (around 0.15) in all three images, we assume that albedo values are correct within ±0.05. This assumption is also justified by a comparison of the albedo from several water bodies (outside the test region) in all three years, which differ by only 0.03 at maximum.

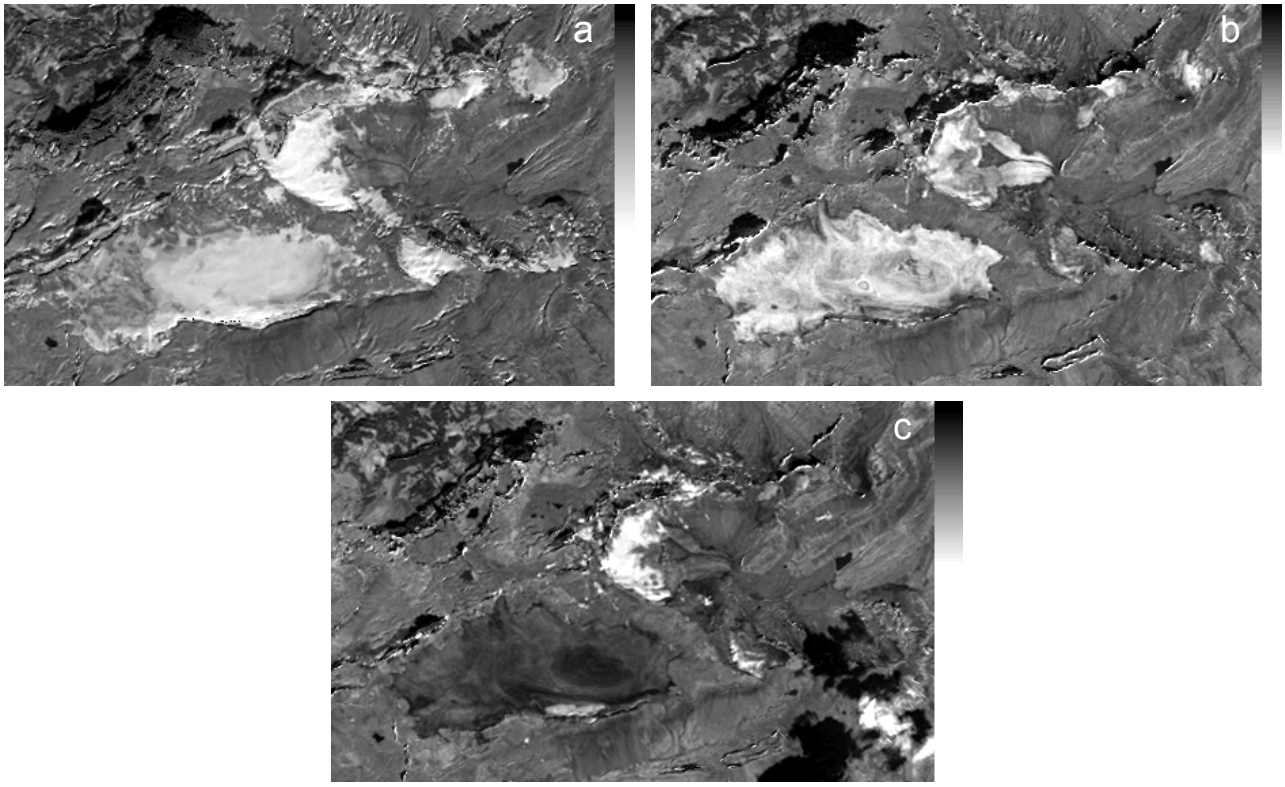

Figure 2: Broadband albedo values for the Wildstrubel test site in the three investigated years: a) 1985, b) 1998 and c) 2003. For better visibility a linear contrast stretch is applied to all images. The greylevel bar to the right of each image gives albedo values from 0.0 (at top) to 1.0 (at bottom).

Absolute albedo values

A comparison of absolute albedo values as obtained for five glaciers in the three years and averaged over 50 m elevation intervals is presented in the two panels of Figure 3. The three mountain glaciers (Figure 3a) have been selected due to the special characteristics of their albedo profile and to illustrate the very individual changes of the albedo with altitude. The two valley glaciers (Figure 3b) are selected to illustrate the albedo variability for elevations above 3300 m and to show the similarities with the mountain glaciers for elevations below 3000 m.

Mostly, albedo values are lowest within the ablation area, reaching minimum values in 2003 (solid lines) of 0.1 to 0.2 for all five glaciers. They are in general somewhat higher for 1998 (dotted) ranging from 0.15 to 0.25. However, Gries glacier (Figure 3a) has in 1998 (blue dotted) a nearly constant albedo with altitude (0.15-0.2), while there is a strong albedo peak of 0.3 for Diablerets and Plaine Morte glacier at their mean elevation. Towards higher elevations the albedo is strongly decreasing (due to dirty snow) and rising again (due to clean snow). In 2003 we found a decreasing albedo (from 0.2 to 0.15) with altitude for Plaine Morte glacier (red solid line) and an alternating pattern for Diablerets glacier (black solid line), similar to 1998 but shifted. The values for 1985 (dashed lines, Figure 3a) show a rather ‘normal’ increase of albedo with elevation, with highest values still below 0.5.

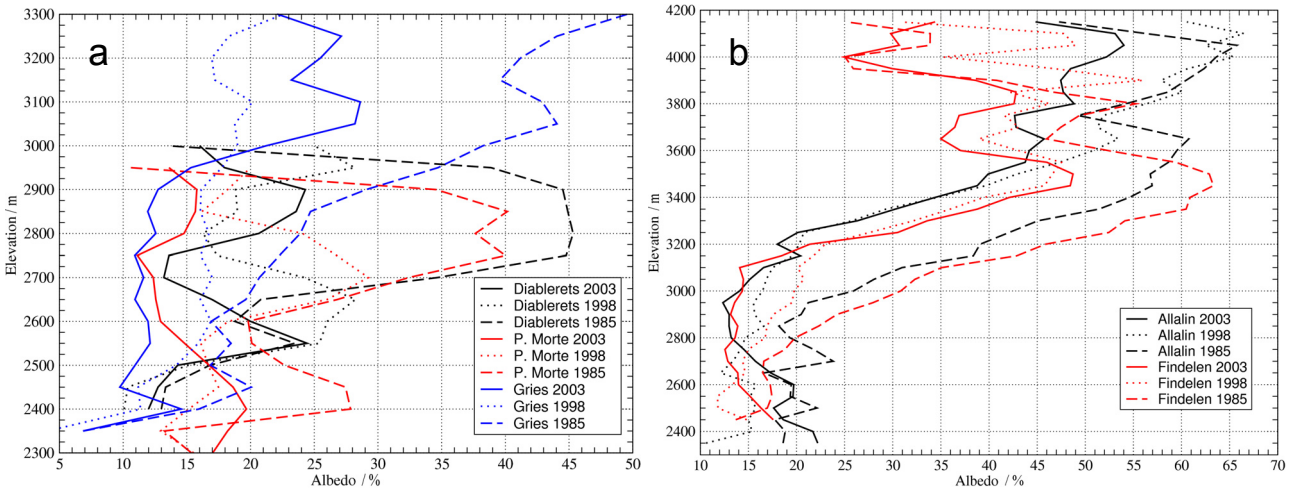

Figure 3: *Albedo values averaged over 50 m elevation intervals for the three investigated years (2003: solid, 1998: dotted, 1985: dashed). a) Three mountain glaciers: Diablerets (black), Plaine Morte (red) and Gries (blue). b) Two valley glaciers: Allalin (black) and Findelen (red).*

Most remarkable for the two valley glaciers depicted in Figure 3b is the decrease of albedo in the ablation area (local minimum of 0.13 around 2900 m) with altitude in 2003 (solid lines) and the comparable low albedo below 3000 m in all three years (from 0.12 to 0.22). In a transition zone from 3200 to 3500 m albedo values are nearly identical for 1998 and 2003, while they exhibit a larger scatter in the snow-covered zone higher up. The sharp drop at the highest glacier points are due to regions in cast shadow that have not been corrected.

Most remarkable for the two valley glaciers depicted in Figure 3b is the decrease of albedo in the ablation area (local minimum of 0.13 around 2900 m) with altitude in 2003 (solid lines) and the comparable low albedo below 3000 m in all three years (from 0.12 to 0.22). In a transition zone from 3200 to 3500 m albedo values are nearly identical for 1998 and 2003, while they exhibit a larger scatter in the snow-covered zone higher up. The sharp drop at the highest glacier points are due to regions in cast shadow that have not been corrected.

Relative changes

In Figure 4 the albedo differences between individual years as obtained by digital subtraction of the respective albedo grids are shown. The colour-coded results are presented together with glacier outlines (thick, black) and elevation contours at 200 m equidistance (thin, black). In order to illustrate albedo changes in another region and for elevations above 3200 m, we have added a second region (Aletsch) for comparison. Apart from deviations due to local artefacts (clouds, cast shadow), significant albedo differences (>0.08) are related to debris-free glacier surfaces. Differences smaller than 0.02 (white) are found widespread in the images, indicating the accuracy of the albedo algorithm.

Comparing 1985 with 1998 in Figure 4a (Wildstrubel test site) the main albedo differences are due to the snow cover that is only present in 1985 (values are up to 0.3 higher in these regions). As mentioned before, bare ice albedos are up to 0.2 higher in 1998 (blue regions). Interestingly, a direct comparison of the snow albedo in both years for higher elevation sites (Figure 4b) reveals higher values in 1998. A direct comparison of 1985 with 2003 (Figures 4c and 4d) gives lower albedo values in 2003 for all regions (apart from slightly lower values over dirty firn in 1985, see Figure 4d), reaching differences of 0.15 over ice and 0.4 over snow.

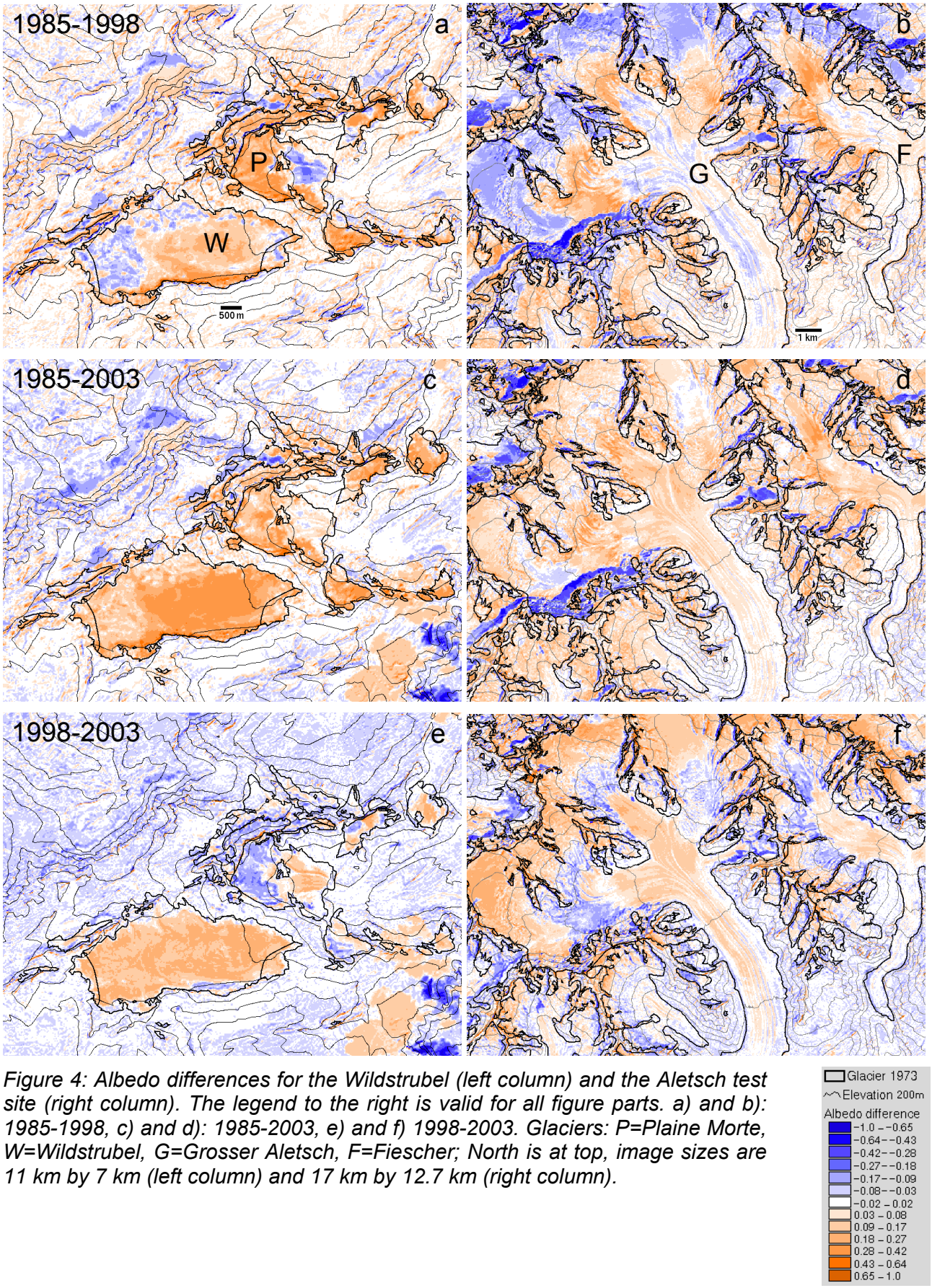

Figure 4: Albedo differences for the Wildstrubel (left column) and the Aletsch test site (right column). The legend to the right is valid for all figure parts. a) and b): 1985-1998, c) and d): 1985-2003, e) and f) 1998-2003. Glaciers: P=Plaine Morte, W=Wildstrubel, G=Grosser Aletsch, F=Fiescher; North is at top, image sizes are 11 km by 7 km (left column) and 17 km by 12.7 km (right column).

Subtracting the 2003 albedo values from the 1998 values (Figures 4e and 4f) shows up to 0.2 lower albedo values in 2003 for the bare ice area (e.g. on Plaine Morte glacier) and up to 0.15 higher albedo values over snow in 2003 (e.g. for Wildstrubel glacier). This dirty snow (or firn) zone is also well recognizable on Grosser Aletsch- (G) and Fiescher glacier (F) in Figure 4f. Higher up, the snow in 1998 is brighter than in 2003. Thus, we find a very complex change of glacier albedo in different zones throughout the three investigated years.

THE DISTRIBUTED GLACIER MASS BALANCE MODEL

The model calculates the mass balance (*MB*) of a glacier from a positive energy balance (*EB*)

$$MB = \sum \left\{ \min\left(0; -\frac{EB}{L}\right) + P_{solid} \right\} \, \mathrm{d}t \,,$$

with

$$EB = (1-\alpha) G f + L_{in} - L_{out} + H_s + H_l$$

Here L is the latent heat of melt, P_{solid} is solid precipitation, α is the albedo, G is the global radiation, f is a factor including cloud cover, L_{in} and L_{out} are the incoming and outgoing longwave radiation fluxes, while H_S and H_l are the sensible and latent heat fluxes, respectively. The physical formulation of the longwave and turbulent fluxes is combined from (8,20,21) and α, G and P are assimilated from gridded data sets that are calculated beforehand. They include TM-derived glacier albedo maps from 1998 and 2003 (the latter increased by 0.05), mean daily potential solar radiation as calculated from the SRAD code (e.g. 22) and climatic means (1971-1990) of annual precipitation sums, which are available at a 2 km grid size (23).

The mean daily temperature (T) is 'distributed' to the terrain by means of gradients (-0.00625 K m^{-1}) for each pixel of the DEM. While L_{in} is calculated from T, the factor f and a constant cloud height (4000 m), L_{out} is held constant (for a 0°C surface). The sensible heat flux H_S depends on T only, while H_l depends also on humidity (calculated from a constant relative humidity of 80% and an elevation (but not time) dependent atmospheric pressure).

Originally the model has been developed to calculate average climatic equilibrium lines and mass balance profiles for several glaciers of a larger catchment from fixed mean climatological parameters. For the purpose of this study we added the possibility to force the model with daily measured values (see below) as well. For both versions the model starts at day number 270 (1 October) and calculates the energy balance components in a loop over all cells of the study area before proceeding with the next day. Glacier melt takes place if the energy balance is positive, solid precipitation falls for T<1.5°C and the satellite derived glacier albedo is used if snow depth is zero. For fresh snow we use a fixed albedo of 0.75 with an exponential ageing curve (8).

For the climatological model run we used the annual mean temperature and its range from Montana (1500 m a.s.l.) with a daily modification prescribed by a shifted sine function (minimum at day 30). Precipitation is resampled to 25 m (cubic interpolation) and increased by 20% (as recommended by (24) for elevations above 1500 m) and falls each 5th day with 1/73 of the annual sum. The global radiation factor f is fixed to 0.5. For the 2002/2003 model run we use averaged time series (daily means) of temperature and global radiation from Montana as well as daily sums of precipitation at Adelboden (1350 m a.s.l.) that are provided by Meteoswiss. The precipitation gradient applied to the DEM is computed from (23). The radiation factor f is calculated by dividing the measured by the potential global radiation as calculated by SRAD for the pixel at the Montana meteo station.

RESULTS OF THE MODELLING

Figure 5 displays the distributed mass balance for the Wildstrubel test site and the four experiments (albedo map 1998 and 2003 combined with a mean climatic and the 2002/3 balance year forcing). While the overall pattern is strongly correlated with the radiative forcing, details are governed by the albedo. The low 2003 albedo (Figures 5b and d) has caused an increase of mass loss with elevation.

Although the absolute mass loss seems to be overestimated in all four experiments (reaching -8 m in the accumulation area, Figure 5d), the general pattern agrees quite well with the observation. While Plaine Morte glacier is, apart from its somewhat shaded highest elevations, free of snow, about one half of Wildstrubel glacier is snow covered (Figure 1c and Figure 5a). Using the 1998 albedo maps (Figures 5a and c), Wildstrubel glacier shows a more or less regular mass balance distribution, which is also visible in the mass balance profiles presented in Figure 6a (green lines). For Plaine Morte glacier there is a strong decrease in mass balance for its flattest parts (red lines), which receive high amounts of solar radiation. The decrease is somewhat less pronounced for climatic mean conditions (dash-dotted red line in Figure 6a).

The low 2003 glacier albedo has disturbed the mass balance profile of both glaciers (black and blue lines in Figure 6a) independent of the meteorological forcing. The less negative mass balance values for Plaine Morte glacier at 2400 and 2900 m (at 2800 m for Wildstrubel glacier) mainly result from local shading effects (see the 'band' of positive values in the middle part of Wildstrubel glacier in Figures 5b and d). In the case of Plaine Morte glacier the positive values cover only a very small fraction of the glacier surface, as obvious from the area-elevation distribution given in Figure 6b (blue bars). The hypsography also indicates that Plaine Morte glacier has no area above 2900 m, which is the major source of accumulation for Wildstrubel glacier (snow covered in Figure 1).

The net balances obtained for the experiment in Figure 5a (climatic mean forcing, albedo 1998) indicate that neither Plaine Morte (-1.7 m) nor Wildstrubel glacier (-0.7 m) is in balance with the 1971- 1990 climatic conditions. However, we did not account for the end of summer 1997 snow conditions (distribution and depth) in our simulation and used the end of summer albedo for the entire melt period. If both effects are taken into account, less negative balances will result. Nevertheless, for Plaine Morte glacier rapid further down-wasting can be expected under present climatic conditions.

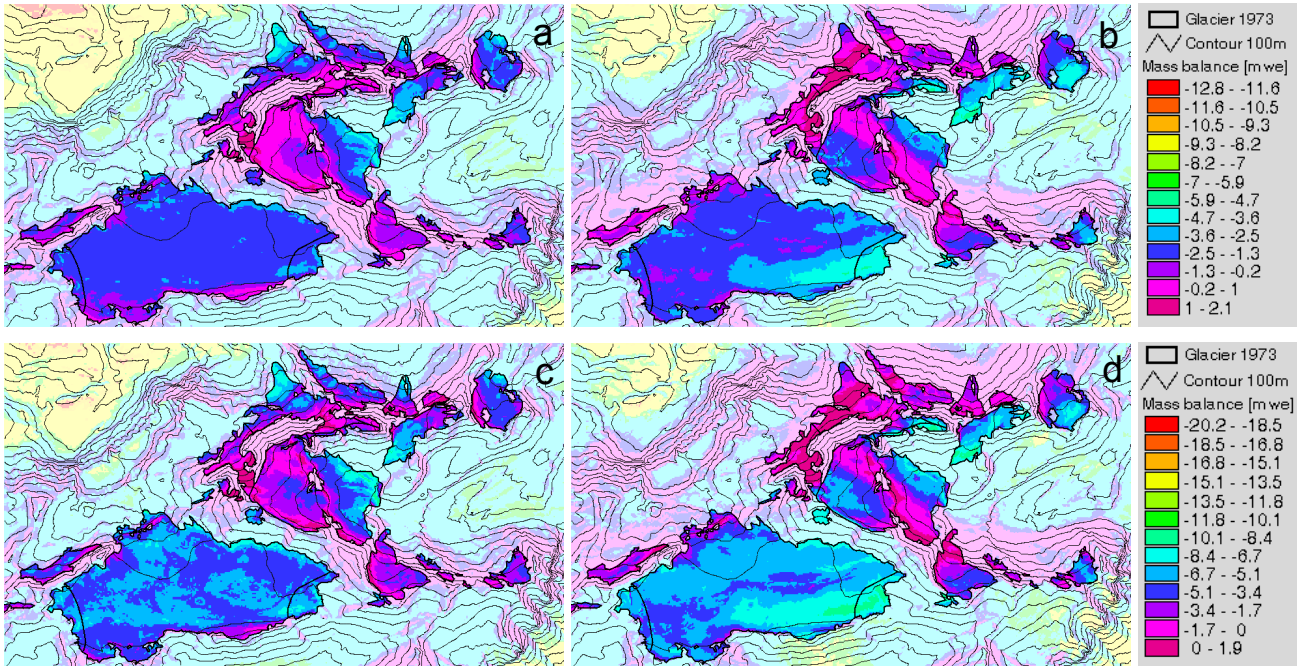

Figure 5: Glacier mass balance distribution as obtained from the model. a) and b) using climatic mean meteorological conditions and the 1998 and 2003 albedo maps, respectively. c) and d) using a daily forcing for the 2002/2003 balance year and the 1998 and 2003 albedo maps, respectively. The colours given in the legends refer to the maps in the same line and are also valid for the less saturated colours outside of glaciers.

There is little change of net balance for the two albedo maps (1998/2003) and identical meteorological forcing (e.g. for 2002/3 conditions: -3.0/-3.1 m for Wildstrubel and -4.9/-5.6 m for Plaine Morte glacier, respectively). However, net balances are about three times less negative for mean

climatic conditions (see above), indicating that the extreme summer 2003 conditions play an important role for the extremely negative mass balances observed.

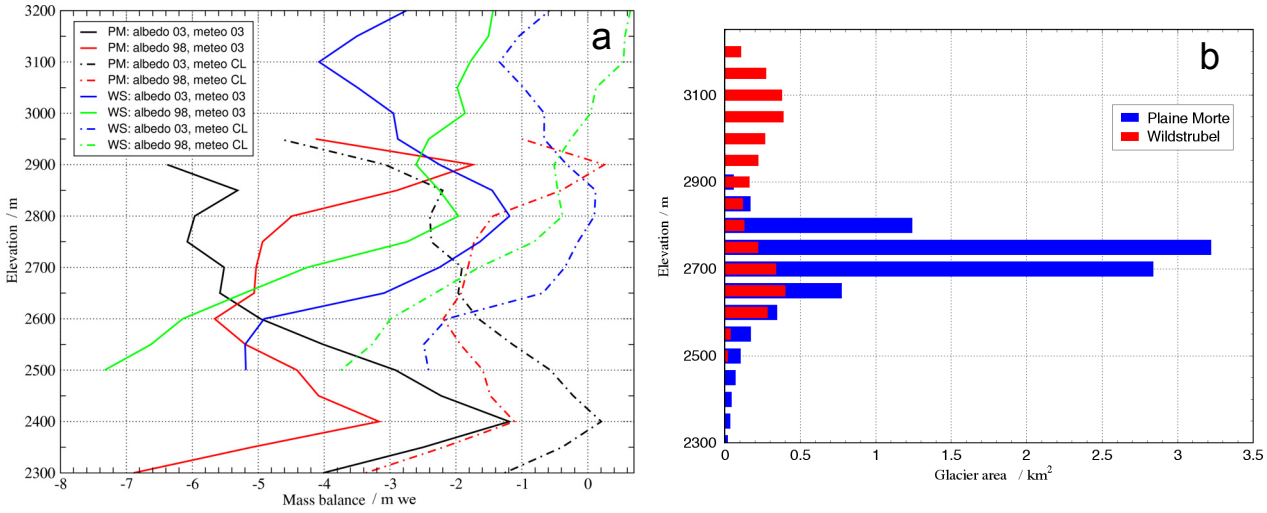

Figure 6: a) Mass balance profiles (mean values for 50 m elevation steps) as obtained for the four model experiments depicted in Figure 5 and the two glaciers Plaine Morte (PM) and Wildstrubel (WS). b) Area-elevation distribution (hypsography) for both glaciers sampled at 50 m elevation bins.

DISCUSSION AND CONCLUSIONS

Although we make some rough assumptions for our broadband albedo calculation of ice and snow, we suggest that the values obtained are correct within 0.05 (little change over other terrain, values for bare rock are correct). As the TM band 2 reflection is very sensitive to impurities and the TM band 4 reflection to the liquid water content, we assume that the very low 2003 albedo in the ablation area is due to a combination of both effects. As the 2003 image was acquired at the end of the second heat wave in August (reaching 26 °C in Montana at the time of the satellite overpass), large amounts of liquid-water might have covered the glacier surface. In 1998, some snow areas are darker than the bare ice regions. Although this is not a general feature, this observation indicates that simple albedo-elevation parameterizations may not be valid in specific years. This conclusion is confirmed by the strong year to year variations observed.

We are not satisfied with the magnitude of the mass balance values obtained from the model, they are too negative. However, several local effects are not yet accounted for (e.g. redistribution of snow by wind, initial snow depth) and seem to play an important role for the initial snow accumulation pattern, which we have also neglected. Still, some general features agree well with the observations and the expected high sensitivity of the mass balance of Plaine Morte glacier can be confirmed. As such, the increasing mass loss towards higher elevations might be realistic under extreme climatic conditions. A validation of the model from measured mass balance values (e.g. for Gries glacier) will be most useful to confirm the results of this study and will be performed in the future.

Some of our more general conclusions are: (i) Albedo of glacier ice and snow can be highly variable from year to year. If glacier mass balance is computed from mass balance models over larger catchments, actual satellite data from the end of the ablation period should be used as an input. The model should also account for an ice-albedo ageing, starting with somewhat higher values at the beginning of the ablation period, as well as an initial snow depth map from the previous year. (ii) Under extreme climatic conditions, glaciers can loose more mass in their accumulation area than in their (shaded) ablation area, inverting a normal mass balance profile. This has to be considered if ablation stake measurements are interpreted, or simple degree-day models are used to calculate glacier melt. (iii) The potential solar radiation governs the mass balance distribution in the case of low glacier albedo and long melt periods. In the rough topography of the Alps an accurate calculation of global radiation from a high-resolution DEM is mandatory.

ACKNOWLEDGEMENTS

This study is supported by grants from COST Action 719 *The use of GIS in climatology and meteorology* (BBW C001.0041) and the EU-funded project ALP-IMP *Multi-centennial climate variability in the Alps based on Instrumental data, Model simulations and Proxy data* (EVK-CT-2002-00148).. Moreover, the study is supported by a grant from the Swiss National Science Foundation (21-105214/1). We are indebted to the careful review of an anonymous referee, who helped to clarify and improve the manuscript considerably.

REFERENCES

1 Singh P & L Bengtsson, 2004. Hydrological sensitivity of a large Himalayan basin to climate change. Hydrological Processes, 18(13): 2363-2385

2 Viviroli D, R Weingartner & B Messerli, 2003. Assessing the hydrological significance of the world's mountains. Mountain Research and Development, 23(1): 32-40

3 Braun L N, M Weber & M Schulz, 2000. Consequences of climate change for runoff from Alpine regions. Annals of Glaciology, 31: 19-25

4 Schär C, P L Vidale, D Lüthi, C Frei, C Häberli, M Liniger & C Appenzeller, 2004. The role of increasing temperature variability in European summer heatwaves. Nature, 427: 332-336

5 Hoelzle M, W Haeberli, M Dischl & W Peschke, 2003. Secular glacier mass balances derived from cumulative glacier length changes. Global and Planetary Change, 36(4): 295-306

6 Arnold N S, I C Willis, M J Sharp, K S Richards & W J Lawson, 1996. A distributed surface energy-balance model for a small valley glacier. I. Development and testing for Haut Glacier d'Arolla, Valais, Switzerland. Journal of Glaciology, 42(140): 77-89

7 Brock B W, I C Willis, M J Sharp & N S Arnold, 2000. Modelling seasonal and spatial variations in the surface energy balance of Haut Glacier d'Arolla, Switzerland. Annals of Glaciology, 31: 53-62

8 Klok E J & J Oerlemans, 2002. Model study of the spatial distribution of the energy and mass balance of Morteratschgletscher, Switzerland. Journal of Glaciology, 48(163): 505-518

9 Escher-Vetter H, 2000. Modelling meltwater production with a distributed energy balance method and runoff using a linear reservoir approach - results from Vernagtferner, Oetztal Alps, for the ablation seasons 1992 to 1995. Zeitschrift für Gletscherkunde und Glazialgeologie, 36: 119-150

10 Greuell W, W H Knap & P C Smeets, 1997. Elevational changes in meteorological variables along a mid-latitude glacier during summer. Journal of Geophysical Research, 102(D22): 25941-25954

11 Strasser U, J Corripio, F Pellicciotti, P Burlando, B Brock & M Funk, 2004. Spatial and temporal variability of meteorological variables at Haut Glacier dArolla (Switzerland) during the ablation season 2001: Measurements and simulations. Journal of Geophysical Research, 109: D03103

12 Oerlemans J, 2000. Analysis of a 3 year meteorological record from the ablation zone of Morteratschgletscher, Switzerland: energy and mass balance. Journal of Glaciology, 46(155): 571-579

13 Knap W H, C H Reijmer & J Oerlemans, 1999. Narrowband to broadband conversion of Landsat-TM glacier albedos. International Journal of Remote Sensing, 20(10): 2091-2110

14 Sandmeier S & K I Itten, 1997. A physically-based model to correct atmospheric and illumination effects in optical satellite data of rugged terrain. IEEE Transactions on Geoscience and Remote Sensing, 35(3): 708-717

15 Vermote E F, D Tanré, J L Deuzé, M Herman & J J Morcrette, 1997. Second simulation of the satellite signal in the solar spectrum, 6S: An overview. IEEE Transactions on Geoscience and Remote Sensing, 35(3): 675-686

16 Greuell J W, C H Reijmer & J Oerlemans, 2002. Narrowband to broadband albedo conversion for glacier ice and snow based on measurements from aircraft. Remote Sensing of Environment, 82: 48-63

17 Greuell W & M S de Ruyter de Wildt, 1999. Anisotropic reflection by melting glacier ice: Measurements and parametrizations in Landsat TM bands 2 and 4. Remote Sensing of Environment, 70: 265-277

18 Paul F & A Kääb, 2005. Perspectives on the production of a glacier inventory from multispectral satellite data in the Canadian Arctic: Cumberland Peninsula, Baffin Island. Annals of Glaciology, 42 (in press)

19 Gratton D J, P J Howarth & D J Marceau, 1993. Using Landsat-5 Thematic Mapper and digital elevation data to determine the net radiation field of a mountain glacier. Remote Sensing of Environment, 43: 315-331

20 Oerlemans J, 1991. A model for the surface balance of ice masses: Part I: alpine glaciers. Zeitschrift für Gletscherkunde und Glazialgeologie, 27/28: 63-83

21 Oerlemans J, 1992. Climate sensitivity of glaciers in southern Norway: application of an energy- balance model to Nigardsbreen, Hellstugubreen and Alfotbreen. Journal of Glaciology, 38(129): 223-232

22 Wilson J P & J C Gallant, 2000. Terrain Analysis: Principles and Applications (Wiley, New York) 512 pp.

23 Schwarb M, C Daly, C Frei & C Schär, 2001. Mean annual precipitation in the European Alps 1971-1990. Hydrological Atlas of Switzerland, Landeshydrologie und Geologie, Bern, Plate 2.6; http://hydrant.unibe.ch/hades/tafel26/tafel26_en.htm

24 Frei C & C Schär, 1998. A precipitation climatology of the Alps from high-resolution rain-gauge observations. International Journal of Climatology, 18(8): 873-900